Microbial Biosynthesis of Alkanes

Andreas Schirmer *et al.*

Science **329**, 559 (2010);
DOI: 10.1126/science.1187936

smallest algae in the Canada Basin, potentially favoring carbon retention and CO_2 release (*19*). However, it is difficult to predict the net role of increased stratification versus sustained wind mixing in these newly ice free regions. Wind-driven upwelling and mixing of nutrient and CO_2 rich subsurface water is expected or already has been shown to have a major impact on carbon dynamics and ecosystem in the Arctic (*21*) or Antarctic (*22*) marginal areas. Such an impact is likely small in the central Canada Basin where increased stratification is a dominant feature (fig. S3).

In addition, warmer temperatures likely would enhance microbial respiration of organic carbon, potentially reducing net community production (*23*). Moreover, increased warming also would promote permafrost thawing and coastal erosion in the Arctic continents, increasing riverine inputs of organic carbon (*24*, *25*) that is subsequently metabolized to CO_2, thus further contributing to the elevated pCO_2. Finally, in future years, when sea surface temperature further increases after all ice is melted during summertime, as is predicted to occur within 30 years (*9*), the Arctic Ocean basin CO_2 uptake capacity would reduce further because of the warming effect on surface-water pCO_2.

The observed summer 2008 pCO_2 distribution suggests that, as ice continues to melt in the near future, the air-sea CO_2 flux will be enhanced in the Arctic Ocean owing to the increased area of open water and longer period of ice-free time. The increase in surface-water pCO_2 due to this CO_2 uptake would accelerate the negative impact of ocean acidification on pelagic and benthic ecosystems. However, the CO_2 uptake would quickly weaken because surface-water pCO_2 will equilibrate with the atmosphere within a short time owing to a shallow mixed-layer depth, strong surface-water stratification, surface warming, and low biological CO_2 fixation.

References and Notes

1. S. Solomon *et al.*, *Climate Change 2007: The Physical Science Basis: Contribution of Working Group I to the Fourth Assessment Report of the Intergovernmental Panel on Climate Change* (Cambridge Univ. Press, Cambridge, 2007).
2. M. Steinacher, F. Joos, T. L. Frölicher, G.-K. Plattner, S. C. Doney, *Biogeosciences* **6**, 515 (2009).
3. M. Yamamoto-Kawai, F. A. McLaughlin, E. C. Carmack, S. Nishino, K. Shimada, *Science* **326**, 1098 (2009).
4. L. G. Anderson, K. Olsson, M. Chierici, *Global Biogeochem. Cycles* **12**, 455 (1998).
5. N. R. Bates, *J. Geophys. Res.* **111**, C10013 (2006).
6. N. R. Bates, J. T. Mathis, *Biogeosciences* **6**, 2433 (2009).
7. K. R. Arrigo, G. L. van Dijken, S. Pabi, *Geophys. Res. Lett.* **35**, L19603 (2008).
8. J. C. Comiso, C. L. Parkinson, R. Gersten, L. Stock, *Geophys. Res. Lett.* **35**, L01703 (2008).
9. M. Wang, J. E. Overland, *Geophys. Res. Lett.* **36**, L07502 (2009).
10. A. Murata, T. Takizawa, *Cont. Shelf Res.* **23**, 753 (2003).
11. S. Kaltin, L. G. Anderson, *Mar. Chem.* **94**, 67 (2005).
12. A. Fransson, M. Chierici, Y. Nojiri, *Cont. Shelf Res.* **29**, 1317 (2009).
13. L. Chen, Z. Gao, *Deep Sea Res. Part II Top. Stud. Oceanogr.* **54**, 2619 (2007).
14. L. A. Codispoti, C. N. Flagg, J. H. Swift, *Deep Sea Res. Part II Top. Stud. Oceanogr.* **56**, 1144 (2009).
15. S. Rysgaard, R. N. Glud, M. K. Sejr, J. Bendtsen, P. B. Christensen, *J. Geophys. Res.* **112**, C03016 (2007).
16. S. Pabi, G. L. van Dijken, K. R. Arrigo, *J. Geophys. Res.* **113**, C08005 (2008).
17. M. Gosselin, M. Levasseur, P. A. Wheeler, R. A. Horner, B. C. Booth, *Deep Sea Res. Part II Top. Stud. Oceanogr.* **44**, 1623 (1997).
18. J. M. Grebmeier, S. E. Moore, J. E. Overland, K. E. Frey, R. Gradinger, *EOS* **91**, 161 (2010).
19. W. K. W. Li, F. A. McLaughlin, C. Lovejoy, E. C. Carmack, *Science* **326**, 539 (2009).
20. R. Gradinger, *Deep Sea Res. Part II Top. Stud. Oceanogr.* **56**, 1201 (2009).
21. E. Carmack, D. C. Chapman, *Geophys. Res. Lett.* **30**, 1778 (2003).
22. M. Montes-Hugo *et al.*, *Science* **323**, 1470 (2009).
23. P. L. Yager, J. W. Deming, *Limnol. Oceanogr.* **44**, 1882 (1999).
24. L. Guo, R. W. MacDonald, *Global Biogeochem. Cycles* **20**, GB2011 (2006).
25. D. A. Hansell, D. Kadko, N. R. Bates, *Science* **304**, 858 (2004).

26. We thank R. Wanninkhof, P. Yager, and N. Bates for discussions; J. Zhao for the salinity and temperature data; and H. Li and S. Gao for sample collection. Funding for the CHINARE CO_2 survey and subsequent synthesis was provided by the Ministry of Science and Technology of China (2009DFA22920), the Natural Science Foundation of China (40531007), and the U.S. National Oceanic and Atmospheric Administration (NA05OAR4311161 and NA09OAR4310078) and NSF (ARC-0909330). The measurements for primary production of phytoplankton were funded by a Korean Arctic Research project (PM09020). We also thank the Chinese Arctic and Antarctic Administration and the Polar Research Institute of China for their support. We are grateful to the captain and crew of icebreaker *Xuelong*.

Supporting Online Material

www.sciencemag.org/cgi/content/full/science.1189338/DC1
Materials and Methods
SOM Text
Figs. S1 to S3
Tables S1 and S2
References

9 March 2010; accepted 28 June 2010
Published online 22 July 2010;
10.1126/science.1189338
Include this information when citing this paper.

Microbial Biosynthesis of Alkanes

Andreas Schirmer,* Mathew A. Rude, Xuezhi Li, Emanuela Popova, Stephen B. del Cardayre

Alkanes, the major constituents of gasoline, diesel, and jet fuel, are naturally produced by diverse species; however, the genetics and biochemistry behind this biology have remained elusive. Here we describe the discovery of an alkane biosynthesis pathway from cyanobacteria. The pathway consists of an acyl–acyl carrier protein reductase and an aldehyde decarbonylase, which together convert intermediates of fatty acid metabolism to alkanes and alkenes. The aldehyde decarbonylase is related to the broadly functional nonheme diiron enzymes. Heterologous expression of the alkane operon in *Escherichia coli* leads to the production and secretion of C13 to C17 mixtures of alkanes and alkenes. These genes and enzymes can now be leveraged for the simple and direct conversion of renewable raw materials to fungible hydrocarbon fuels.

Efforts to transition from fossil fuels to renewable alternatives have focused on the conversion of renewable biomass to "drop-in" compatible fuels and chemicals (*1*–*3*). Routes to renewable hydrocarbons are emerging, but to date, these require expensive chemical hydrogenation. Alkanes, observed throughout nature, are produced directly from fatty acid metabolites—for example, as plant cuticular waxes (*4*), as insect pheromones (*5*), and with unknown functions in numerous organisms (*6*–*9*). Biochemical studies of alkane biosynthesis have focused on eukaryotic systems, with most evidence supporting a decarbonylation of fatty aldehydes as the primary mechanism (*10*, *11*). Although *cer1* from *Arabidopsis thaliana* has been proposed as a candidate gene encoding this activity (*12*), no studies conclusively associate any gene with these biochemical activities.

Alkanes have been reported in a diversity of microorganisms, but some results remain controversial (*13*, *14*). From our assessment, the most consistent reports are from the cyanobacteria (*9*, *15*, *16*) and natural habitats dominated by cyanobacteria (*17*). Heptadecane is the most abundant alkane reported in these photoautotrophic bacteria, an observation consistent with the "$n-1$" rule for alkanes, resulting from decarbonylation of typically even-numbered fatty aldehydes. Because cyanobacteria are phylogenetically homogeneous, with more than 50 sequenced genomes publicly available, our search began with comparative biochemistry and genomics. Eleven cyanobacterial strains of known sequence were photoautotrophically grown, and their culture extracts were evaluated for hydrocarbon production (Table 1). Ten of these strains produced alkanes, mainly heptadecane and pentadecane, along with alkenes, presumably derived from unsaturated fatty aldehydes. However, one strain, *Synechococcus* sp. PCC7002, did not produce alkanes. On the assumption that an alkane biosynthesis pathway was not present in *Synechococcus* sp. PCC7002, we undertook a subtractive genome analysis. The 10 genomes of the alkane-producing cyanobacteria were intersected, and the PCC7002 genome was subtracted by using a 40% sequence identity cut-off to select orthologs. Seventeen genes common to the 10 producing strains remained, and 10 of these already had assigned

LS9, Inc., 600 Gateway Boulevard, South San Francisco, CA 94080, USA.

*To whom correspondence should be addressed. E-mail: aschirmer@ls9.com

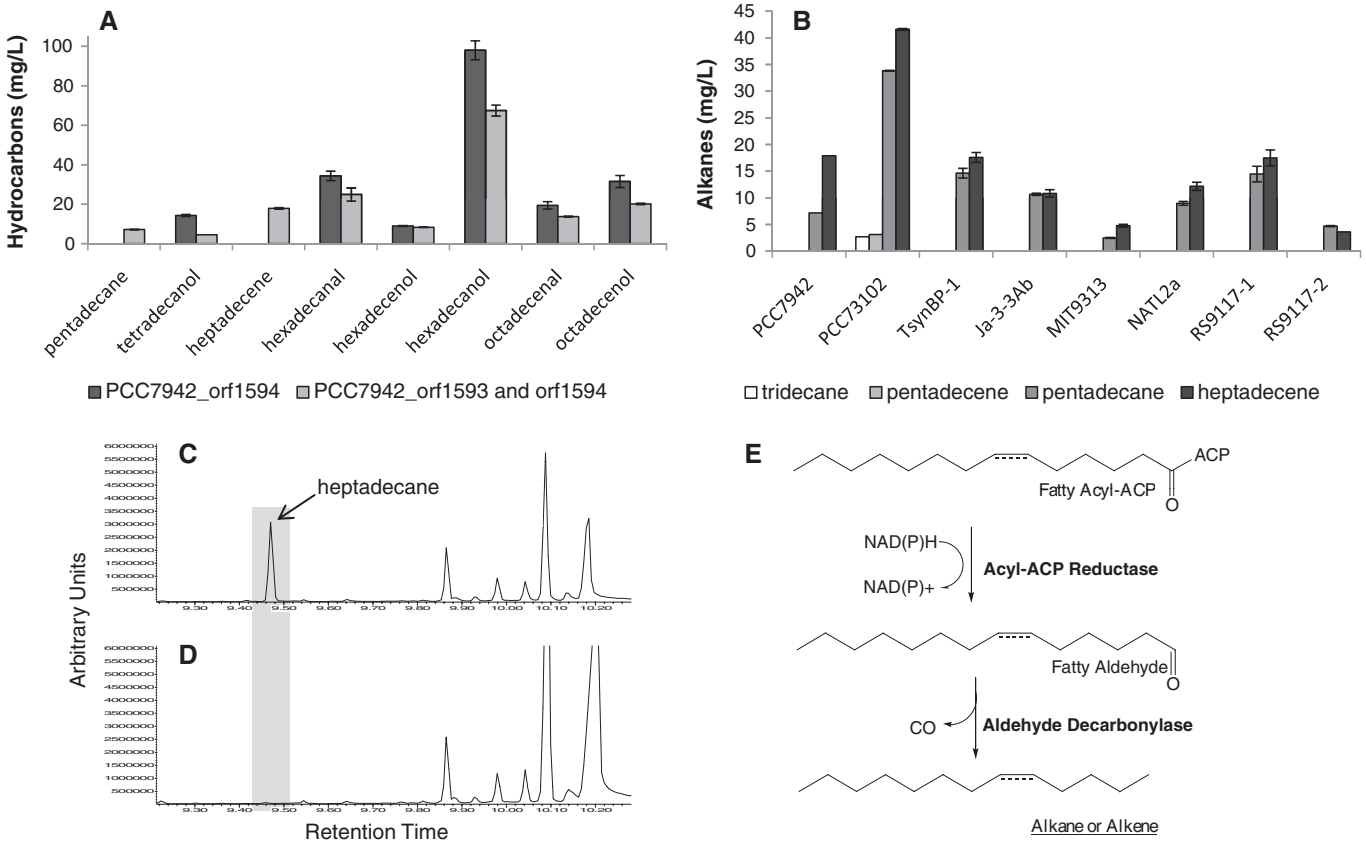

Fig. 1. Demonstration that a two-gene pathway widespread in cyanobacteria is responsible for alkane biosynthesis. (**A**) *E. coli* MG1655 does not produce hydrocarbons. When *S. elongatus* PCC7942_orf1594 was expressed, *E. coli* produced fatty aldehydes and fatty alcohols. The coexpression of *S. elongatus* PCC7942_orf1593 and orf1594 led to alkane, alkene, fatty aldehyde, and fatty alcohol production. (**B**) For comparison, selected PCC7942_orf1593 orthologs from other cyanobacteria were coexpressed with PCC7942_orf1594 in *E. coli*, and all produced similar compounds [only alkanes and alkenes are shown; fig. S1 shows an example of a detailed gas chromatography–mass spectrometry (GC-MS) trace of a recombinant hydrocarbons mixture]. (**C**) *Synechocystis* sp. PCC6803 has the ability to synthesize the alkane heptadecane. (**D**) Deletion of the two adjacent *Synechocystis* sp. PCC6803 orfs sll0208 and sll0209, *S. elongatus* PCC7942_orf1593 and 1594 orthologs, abolished heptadecane biosynthesis. GC-MS traces are shown. (**E**) Model of the alkane biosynthesis pathway in cyanobacteria consisting of a fatty aldehyde–generating acyl-ACP reductase (e.g., PCC7942_orf1594 or sll0209) and a fatty aldehyde decarbonylase (e.g., PCC7942_orf1593 or sll0208). The PCC7942_orf1593 orthologs in (B) are from the following strains: *N. punctiforme* PCC73102, *Thermosynechococcus elongatus* BP-1, *Synechococcus* sp. Ja-3-3Ab, *P. marinus* MIT9313, *P. marinus* NATL2A, and *Synechococcus* sp. RS9117, which has two paralogs (RS9117-1 and -2).

functions (table S2). Two of the remaining hypothetical proteins stood out as likely candidates for alkane biosynthesis. Representative of these were open reading frames orf1593 and orf1594 from *S. elongatus* PCC7942. PCC7942_orf1594 belongs to the short-chain dehydrogenase or reductase family, whereas PCC7942_orf1593 shared similarity to the ferritin-like or ribonucleotide reductase–like family. Because alkane biosynthesis was predicted to proceed via the decarbonylation of fatty aldehydes, it was possible that PCC7942_orf1594 catalyzed the reduction of a fatty acid intermediate, such as an acyl carrier protein (ACP) or coenzyme A (CoA) acyl-thioester, to form a fatty aldehyde (*18*, *19*), and that PCC7942_orf1593, which is similar to enzymes that catalyze radical-based chemical reactions such as ribonucleotide reductase R2 (*20*), was the decarbonylase. PCC7942_orf1593 and orf1594 orthologs appear to occur only in cyanobacteria and likely form a conserved operon, because they are found adjacent to each other in a majority of cyanobacterial genomes (table S3). *Cyanothece* sp. PCC7424 was the only additional strain identified that lacked orthologs to these sequences.

Table 1. Occurrence of alkanes in selected cyanobacteria with fully sequenced genomes (*21*).

Cyanobacterium	Genome size (Mb)	Hydrocarbons previously reported	Alkanes observed in this study
Synechococcus elongatus PCC7942	2.7	Yes*	Heptadecane, pentadecane
S. elongatus PCC6301	2.7	Yes*	Heptadecane, pentadecane
Synechocystis sp. PCC6803	3.5	Not reported	Heptadecane
Prochlorococcus marinus CCMP1986	1.7	Not reported	Pentadecane
Anabaena variabilis ATCC29413	6.4	Yes†	Heptadecane, methyl-heptadecane
Nostoc punctiforme PCC73102	9.0	Not reported	Heptadecane
Gloeobacter violaceus PCC7421	4.6	Not reported	Heptadecane
Nostoc sp. PCC7120	6.2	Not reported	Heptadecane, methyl-heptadecane
Cyanothece sp. PCC7425	5.7	Not reported	Heptadecane
Cyanothece sp. ATCC51142	4.9	Not reported	Pentadecane
Synechococcus sp. PCC7002	3.0	Yes*	No alkanes observed

*From (*9*), in which *S. elongatus* and *Synechococcus* sp. PCC7002 are listed under their former names *Anacystis nidulans* and *Agmenellum quadruplicatum*, respectively. †From (*26*).

To test the hypothesis that the *S. elongatus* PCC7942_orf1593 and orf1594 family proteins were necessary and sufficient for alkane biosynthesis, a genetic "knock in" and "knock out" strategy was taken. PCC7942_orf1593 and orf1594 were expressed both separately and together in *Escherichia coli*, and extracts of these cells were evaluated for the production of hydrocarbons.

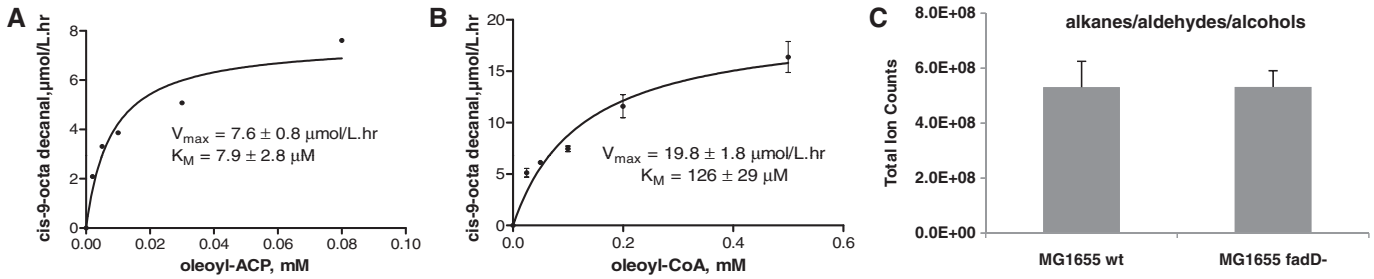

Fig. 2. Demonstration that *S. elongatus* PCC7942_orf1594 encodes an acyl-ACP reductase. (**A** and **B**) Michaelis-Menten plots for PCC7942_orf1594 protein with oleoyl-ACP and oleoyl-CoA as substrates. NADPH concentration was 2 mM. (**C**) Comparison of hydrocarbon production of *E. coli* wild-type and an *E. coli fadD* deletion strain. Both strains express *S. elongatus* PCC7942_orf1593 and orf1594. *fadD* encodes the major acyl-CoA synthetase of *E. coli*. As this strain lacks the ability to synthesize acyl-CoAs, hydrocarbons are derived directly from acyl-ACP.

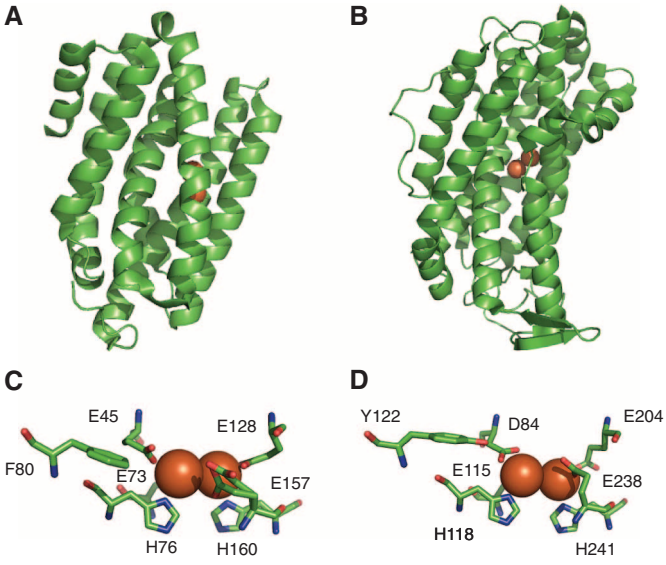

Fig. 3. Comparison of the similar three-dimensional structures of a cyanobacterial aldehyde decarbonylase and ribonucleotide reductase R2 from *E. coli*. (**A**) Aldehyde decarbonylase from *P. marinus* MIT9313 from PDB file 2OC5. (**B**) Ribonucleotide reductase R2 from *E. coli* from PDB file 1RIB. (**C**) Active site of the *P. marinus* MIT9313 aldehyde decarbonylase. (**D**) Active site of the *E. coli* ribonucleotide reductase R2. Amino acid residues that coordinate the metal centers are shown. The active site of *E. coli* ribonucleotide reductase R2 also shows a tyrosine, which is part of the diiron(III)–tyrosyl radical cofactor and which is replaced with a phenylalanine in the aldehyde decarbonylase structure. The structure of *P. marinus* MIT9313 aldehyde decarbonylase shows two iron atoms bound, but it cannot be excluded that the active enzyme is a manganese/iron protein (see text). Structures were viewed in PyMOL.

Although *E. coli* produced no detectable hydrocarbons, extracts of PCC7942_orf1594-expressing cells contained substantial quantities of even-chain fatty aldehydes and fatty alcohols (Fig. 1A), whereas coexpression of both PCC7942_orf1593 and orf1594 resulted in the production of odd-chain alkanes and alkenes, as well as even-chain fatty aldehydes and fatty alcohols (Fig. 1A). Thus, PCC7942_orf1593 and orf1594 are sufficient for in vivo alkane biosynthesis, and fatty aldehydes are likely the biosynthetic intermediates. Expression of PCC7942_orf1593 alone was indistinguishable from the *E. coli* negative control, which was expected, because *E. coli* does not naturally produce fatty aldehydes. The production of fatty alcohols upon PCC7942_orf1594 expression can be attributed to intrinsic activities in *E. coli* that reduce fatty aldehydes to fatty alcohols, as is observed upon expression of fatty acyl-CoA reductases (*19*). Although it is possible that fatty alcohols may be biosynthetic intermediates, for mechanistic reasons it seems unlikely, and in vitro experiments support this hypothesis (see below). Fifteen additional PCC7942_orf1593 orthologs from various cyanobacteria were evaluated (table S3), and all conferred alkane production when expressed in *E. coli* together with PCC7942_orf1594. Alkane profiles of selected strains in Fig. 1B show that the "recombinant hydrocarbon" mixtures are primarily made up of pentadecane and heptadecene. Strains with the highest titers, e.g., coexpressing the orf1593 orthologs from *Nostoc punctiforme* PCC73102, produced a mixture of tridecane, pentadecene, pentadecane, and heptadecene, typically at a ratio of 10:10:40:40. Alkane titers were over 300 mg/liter when a modified mineral medium was used (*21*), and more than 80% of the hydrocarbons were found outside the cells (fig. S2).

In *S. elongatus* PCC7942, orf1593 and orf1594 appear to be part of a larger operon that contains a gene encoding a subunit of the acetyl-CoA carboxylase (*accA*), which is essential for growth. To avoid any polar effects of deleting the genes, we replaced the PC7942_orf1593 and 1594 orthologs in *Synechocystis* sp. PCC6803 (where the orthologous genes apparently form only a bicistronic operon) with a kanamycin-resistance cassette. This replacement abolished the presence of alkanes (Fig. 1, C and D) in the extracts of photoautoptrophically grown cells. Thus, these genes are both necessary for alkane biosynthesis in cyanobacteria and sufficient to confer alkane biosynthesis in a heterologous host, such as *E. coli*. Our findings further support the model of odd-chain alkane biosynthesis through the decarbonylation of even-chain fatty aldehydes.

The proposed pathway for alkane biosynthesis is depicted in Fig. 1E. To evaluate this model, we undertook a preliminary in vitro characterization of the purified recombinant enzymes (*21*). Acyl-acyl carrier protein (acyl-ACP) and acyl-coenzyme A (acyl-CoA), the major activated forms of fatty acids in bacteria, were evaluated as substrates for PCC7942_orf1594. When incubated with acyl-ACP or acyl-CoA (e.g., oleoyl-ACP and oleoyl-CoA), PCC7942_orf1594 catalyzed the reduced nicotinamide adenine dinucleotide phosphate ($NADP^+$) (NADPH)–dependent reduction to the corresponding fatty aldehyde (e.g., *cis*-9-octadecenal) and required divalent cations, such as magnesium for catalysis. Fatty alcohols were not observed in the in vitro reaction. Although both fatty acyl thioesters were substrates, the Michaelis constant (K_M) for acyl-ACP was 8 ± 2 µM, and that for acyl-CoA was 130 ± 30 µM (Fig. 2, A and B). Accordingly, we named this enzyme acyl-ACP reductase (AAR), because it appears that acyl ACP is kinetically preferred and is likely the in vivo substrate. This hypothesis is supported by our finding that PCC7942_orf 1593 and orf1594 coexpression in an *E. coli* strain devoid of acyl-CoAs (the major acyl-CoA synthetase gene *fadD* was deleted) led to very similar levels of hydrocarbon production, comparable to those in an *E. coli* wild-type strain (Fig. 2C). This substrate selectivity distinguishes AAR from fatty acyl-CoA reductases (FAR) that specifically reduce acyl-CoAs but not acyl-ACPs to fatty aldehydes (*19*).

Comparison of PCC7942_orf1593 to the sequence database suggested that the cyanobacterial aldehyde decarbonylases are members of the ferritin-like or ribonucleotide reductase–like family of nonheme diiron enzymes (*20*). This was confirmed by a crystal structure of the

PCC7942_orf1593 ortholog from *Prochlorococcus marinus* MIT9313, PMT1231, solved by the Joint Center of Structural Genomics (protein database entry PDB|2OC5|A) but without assigning an enzymatic function. We confirmed that PMT1231, like PCC7942_orf1593, is an active aldehyde decarbonylase, because it conferred alkane biosynthesis to *E. coli* when coexpressed with PCC7942_orf1594 (Fig. 1B). The three-dimensional structure shows similarities to the 8 α-helical bundle of the second subunit of *E. coli* ribonucleotide reductase (R2) (*22*) (Fig. 3, A and B). In the solved structures, both proteins have two irons coordinated to histidine and aspartate or glutamate residues (Fig. 3, C and D). In R2, the diiron is part of a diiron(III)–tyrosyl radical cofactor that is essential to the ribonucleotide reduction process as a radical-chain initiator (*20*). The radical is then transduced to the catalytic R1 subunit. Homology modeling revealed that this tyrosine residue in R2 (Tyr^{122}) was replaced by phenylalanine residues in the aldehyde decarbonylases (e.g., Phe^{80} in PMT1231) (Fig. 3, C and D), which suggested that decarbonylation does not include a diiron(III)–tyrosyl radical cofactor. To examine the possibility that another conserved tyrosine might form such a cofactor in the aldehyde decarbonylases, we replaced a tyrosine, which was conserved in all cyanobacterial decarbonylases and appeared to be within 6 Å of the diiron (e.g., Tyr^{135} in PMT1231), with phenylalanine. This mutation had no detectable effect on alkane biosynthesis activity in vivo (fig. S3), which suggested that decarbonylation proceeds through a mechanism different from ribonucleotide reductase R2. A different class of R2s, exemplified by the R2 from *Chlamydia trachomatis*, is a manganese/iron and not a diiron protein, and it does not use a diiron(III)-tyrosyl but a stable manganese(IV)/iron(III) cofactor for radical initiation (*23*). At present, we cannot exclude that active aldehyde decarbonylases are manganese/iron proteins—heterologous expression in *E. coli* might result in mismetallation. Aldehyde decarbonylases are also considerably smaller than ribonucleotide reductase R2s (220 to 250 versus 300 to 400 amino acids) and lack the C-terminal region that, in R2, interacts with the R1 subunit.

To evaluate in vitro decarbonylation, we tested the purified aldehyde decarbonylase from *Nostoc punctiforme* PCC73102, NpunR1711, which had shown the highest in vivo activity (Fig. 1B), with octadecanal as substrate in the presence or absence of different cofactors. As a number of nonheme diiron enzymes require ferredoxin, ferredoxin reductase, and reducing equivalents for activity (*24*, *25*), we tested commercially available spinach ferredoxin and ferredoxin reductase and NADPH. Indeed, in vitro decarbonylation of octadecanal to heptadecane was only observed in the presence of ferredoxin, ferredoxin reductase, and NADPH, and omitting any one of these cofactors completely abolished in vitro activity of the decarbonylase (fig. S4). As coexpression of a cyanobacterial acyl-ACP reductase and aldehyde decarbonylase is sufficient for in vivo alkane biosynthesis in *E. coli* (see above), ferredoxin and ferredoxin reductase components essential for decarbonylation must be provided at least to some extent by endogenous *E. coli* proteins.

The genes and enzymes described here provide a foundation for the deeper understanding and further development of this pathway. The ability to biologically convert renewable carbohydrate selectively to fuel-grade alkanes without hydrogenation is an important step toward the goal of low-cost renewable transportation fuels.

References and Notes

1. J. L. Fortman *et al.*, *Trends Biotechnol.* **26**, 375 (2008).
2. J. R. Regalbuto, *Science* **325**, 822 (2009).
3. M. A. Rude, A. Schirmer, *Curr. Opin. Microbiol.* **12**, 274 (2009).
4. L. Samuels, L. Kunst, R. Jetter, *Annu. Rev. Plant Biol.* **59**, 683 (2008).
5. J. A. Tillman, S. J. Seybold, R. A. Jurenka, G. J. Blomquist, *Insect Biochem. Mol. Biol.* **29**, 481 (1999).
6. N. Ladygina, E. G. Dedyukhina, M. B. Vainshtein, *Process Biochem.* **41**, 1001 (2006).
7. P. Metzger, C. Largeau, *Appl. Microbiol. Biotechnol.* **66**, 486 (2005).
8. G. A. Strobel *et al.*, *Microbiology* **154**, 3319 (2008).
9. K. Winters, P. L. Parker, C. Van Baalen, *Science* **163**, 467 (1969).
10. T. M. Cheesbrough, P. E. Kolattukudy, *Proc. Natl. Acad. Sci. U.S.A.* **81**, 6613 (1984).
11. M. Dennis, P. E. Kolattukudy, *Proc. Natl. Acad. Sci. U.S.A.* **89**, 5306 (1992).
12. M. G. Aarts, C. J. Keijzer, W. J. Stiekema, A. Pereira, *Plant Cell* **7**, 2115 (1995).
13. T. G. Tornabene, *Experientia* **38**, 43 (1982).
14. L. P. Wackett, J. A. Frias, J. L. Seffernick, D. J. Sukovich, S. M. Cameron, *Appl. Environ. Microbiol.* **73**, 7192 (2007).
15. A. G. McInnes, J. A. Walter, J. L. C. Wright, *Lipids* **15**, 609 (1980).
16. V. M. Dembitsky, M. Srebnik, *Biochemistry (Mosc.)* **67**, 1276 (2002).
17. J. Shiea, S. C. Brassell, D. M. Ward, *Org. Geochem.* **15**, 223 (1990).
18. T. T. P. Doan *et al.*, *J. Plant Physiol.* **166**, 787 (2009).
19. S. Reiser, C. Somerville, *J. Bacteriol.* **179**, 2969 (1997).
20. J. Stubbe, P. Riggs-Gelasco, *Trends Biochem. Sci.* **23**, 438 (1998).
21. Materials and methods are available as supporting material on *Science* Online.
22. P. Nordlund, B. M. Sjöberg, H. Eklund, *Nature* **345**, 593 (1990).
23. W. Jiang *et al.*, *Science* **316**, 1188 (2007).
24. J. Müller, A. A. Lugovskoy, G. Wagner, S. J. Lippard, *Biochemistry* **41**, 42 (2002).
25. C. H. Wu, W. Jiang, C. Krebs, J. Stubbe, *Biochemistry* **46**, 11577 (2007).
26. S. W. Fehler, R. J. Light, *Biochemistry* **9**, 418 (1970).

27. We thank M. Alibhai for homology modeling, S. Brubaker for bioinformatics work, T. Baron for technical assistance, and C. Chang for help with preparing Fig. 3. The patent applications WO 2009/140695 and WO 2009/140696 are relevant to this paper. All authors have a financial interest in LS9, Inc. We would like to dedicate this paper to the memory of C. Richard Hutchinson, who died on 5 January 2010. "Hutch" was an important mentor for A.S. and S.B.d.C. He will be missed.

Supporting Online Material

www.sciencemag.org/cgi/content/full/329/5991/559/DC1
Materials and Methods
Figs. S1 to S4
Tables S1 to S3
References

4 February 2010; accepted 16 June 2010
10.1126/science.1187936

Btbd7 Regulates Epithelial Cell Dynamics and Branching Morphogenesis

Tomohiro Onodera,[1]* Takayoshi Sakai,[1,2]*† Jeff Chi-feng Hsu,[1]* Kazue Matsumoto,[1] John A. Chiorini,[3] Kenneth M. Yamada[1]†

During embryonic development, many organs form by extensive branching of epithelia through the formation of clefts and buds. In cleft formation, buds are delineated by the conversion of epithelial cell-cell adhesions to cell-matrix adhesions, but the mechanisms of cleft formation are not clear. We have identified Btbd7 as a dynamic regulator of branching morphogenesis. Btbd7 provides a mechanistic link between the extracellular matrix and cleft propagation through its highly focal expression leading to local regulation of Snail2 (Slug), E-cadherin, and epithelial cell motility. Inhibition experiments show that Btbd7 is required for branching of embryonic mammalian salivary glands and lungs. Hence, *Btbd7* is a regulatory gene that promotes epithelial tissue remodeling and formation of branched organs.

Branching morphogenesis is a fundamental developmental process generating the branched epithelia of many organs, including lungs, kidneys, and the mammary and salivary glands (*1*–*8*). Branches are generated by local outgrowths or by formation of clefts that subdivide epithelia into buds. Bud or tubule extension is promoted by various growth factors (*9*–*11*), but the mechanism of cleft formation is poorly understood. One model for cleft formation involves the local loss of epithelial cell-cell adhesions and replacement by interactions with extracellular matrix accumulating within clefts (*9*, *12*, *13*).

The matrix protein fibronectin is required for salivary, kidney, and lung branching (*13*–*15*).

[1]Laboratory of Cell and Developmental Biology, National Institute of Dental and Craniofacial Research, National Institutes of Health, Bethesda, MD 20892–4370, USA. [2]Department of Oral-Facial Disorders, Osaka University Graduate School of Dentistry, Yamadaoka, Suita, Osaka 565-0871, Japan. [3]Molecular Physiology and Therapeutics Branch, National Institute of Dental and Craniofacial Research, National Institutes of Health, Bethesda, MD 20892–4370, USA.

*These authors contributed equally to this work.
†To whom correspondence should be addressed. E-mail: sakai@dent.osaka-u.ac.jp (T.S.); kyamada@mail.nih.gov (K.M.Y.)